J. Water Environ. Nanotechnol., 5(4): 294-306 Autumn 2020

ORIGINAL RESEARCH PAPER

Photocatalytic Degradation of Organic Dyes by PEG and PVP Capped Cu, Ni and Ag Nanoparticles in the Presence of $NaBH_4$ in Aqueous Medium

Subramanian Kanchana*, Radhakrishnan Vijayalakshmi

Department of Chemistry, Quaid-E-Millath Government College for Women (Aut.), Chennai-600002, India

Received: 2020-08-05 Accepted: 2020-09-30 Published: 2020-11-15

ABSTRACT

Photocatalysis mediated by metal nanoparticles is emerging as an effective method for the removal of hazardous dye pollutants in natural aquatic bodies. Nanoparticles of Cu, Ni, and Ag were synthesized by chemical methods using PEG and PVP polymers as capping agents. Experimental photocatalysis was carried out in a single pot batch reactor using metal nanoparticle catalysts for the degradation of crystal violet (CV), bromocresol green (BCG), and methylene blue (MB) in an aqueous solution in the presence of $NaBH_4$ reductant independently under solar and UV irradiations at 25°C. Metal nanoparticles caused the removal of BCG and CV in 90-120 min and MB in 30-60 min. A linear relationship between the irradiation time and the absorbance was recorded and the kinetic plots exhibited pseudo-first-order kinetic. The trend of dye degradation among the nanoparticles based on the catalytic efficiency (φ_c) and rate coefficient (k) values was Cu>Ag>Ni. Mineralization experiments indicated 94, 91, and 90% of the TOC removal ratio (R) respectively for CV, MB, and BCG dyes. Nanoparticles stabilized using PEG demonstrated better catalytic efficiency than those with PVP. Solar irradiation showed a superior augmenting effect on the nanoparticle catalysts than the UV irradiation. The electron-hole pair mediated reduction mechanism was proposed as a basis for dyes photocatalytic degradation.

Keywords: *Metal nanoparticles, stabilizers, decolorization, photocatalysis, kinetics*

How to cite this article

Kanchana S., Vijayalakshmi R. Photocatalytic Degradation of Organic Dyes by PEG and PVP Capped Cu, Ni and Ag Nanoparticles in the Presence of $NaBH_4$ in Aqueous Medium. J. Water Environ. Nanotechnol., 2020; 5(4): 294-306.
DOI: 10.22090/jwent.2020.04.001

INTRODUCTION

Rapid population increase, industrialization growth, and indiscriminate urbanization are the main causes of grave irrevocable environmental damages. Industries which manufacture textiles, refineries, paper pulp, pesticides, batteries, etc. discharge several millions of gallons of wastewater daily. The effluent-borne organic pollutants jeopardize the terrestrial and aquatic bodies of the natural environment such as rivers, ponds, lakes, and so on. Organic dyes, that are employed in industries such as paints, textiles, plastics, tannery, and printing industries are complex molecules. Currently, more than 10 million different dyes amounting to $7x10^5$ tones are produced globally every year [1]. Approximately 12-15% of the dyes applied in the manufacturing activities are discharged through the effluent as they are not entirely fixed [2].

In recent years, there is a growing concern about the environmental pollution caused by inadequately treated dye bearing industrial effluents. Most of these dyes are resistant to biodegradation and endanger the living organisms particularly when released in water bodies [3]. Accumulation of intensely colored dyes in water bodies restrict the penetration of sunlight, hinder the circulation of oxygen, promote eutrophication, and eventually compromise the natural trend of aquatic life [4]. Many studies have

* Corresponding Author Email: *skanchana7@gmail.com*

reported the carcinogenic and lethal effects of these dye pollutants to all forms of life due to their infusion into both surface and groundwater bodies [3-6]. When imbibed into the food chain, the dyes comprised of azo and triphenyl methylene groups could cause serious health hazards and multi-organ damages in the human body [7,8].

The presence of dyes poses two critical challenges in treating the contaminated water: One is their chemical complexity which resists faster microbial biodegradation and the other constraint is detecting dyes at low concentrations [3]. Conventional methods of wastewater treatment like adsorption, electrochemical methods, and ultrafiltration, activated carbon and oxidation are rather less effective in complete removal of the dyes, or expensive and more time consuming [9].

More recently, heterogeneous photocatalysis has emerged as an effective method of choice for the remediation of dye polluted water. This eco-friendly method offers complete degradation of organic contaminants with the least energy consumption. Advantages of this method are the conversion of pollutants into non-toxic chemicals and gases, use of natural (solar) energy sources, quick oxidation, no formation of polycyclic products, and no obligation for sludge removal [10-12]. Photocatalytic degradation of pollutants is carried out with the help of semiconductor materials (catalysts) and light energy [13]. Being an oxidative process, heterogeneous photocatalysis employs common energy sources such as UV irradiation (300-400 nm), solar radiation, and visible light for the degradation of pollutants [14]. During the process, valence band holes and conduction band electrons are produced upon the excitation of photocatalyst, caused by high energy radiation. While the ·OH is formed due to the reaction of valence band holes with H_2O and hydroxide ion, the electrons cause the generation of peroxide radicals by reacting with molecular oxygen adsorbed on the catalyst [15,16]. The ·OH free-radicals thus formed react with the organic contaminants and either convert them into nonhazardous substances or degrade completely into CO_2 and H_2O [17].

Studies have demonstrated that catalysts play a substantial role in the photodecomposition of organic pollutants in terms of facilitating the reactions and minimizing the wastes. Therefore, careful selection of catalysts is critical in photocatalytic remediation. The nanoparticles of transition metals, by virtue of their shape, size, specificity, large surface area to volume ratio, and thermodynamic stability, have attracted the attention of researchers in late years for application as potential catalysts. The metal nanoparticles (M-NPs), after activation by sunlight in aqueous solutions, act as sensitizers to enhance the photocatalysis of degradation of pollutants through a light-induced redox mechanism [18]. Transition M-NPs synthesized with synthetic stabilizers such as poly N-vinyl pyrrolidone (PVP) can be tuned through optimizing the experimental conditions for treatment of effluents of chemical and bio-medical industries [19].

Bromocresol Green (BCG), Crystal Violet (CV), and Methylene Blue (MB) are the organic dyes possessing triphenyl methylene functional group. These dyes have found extensive applications in various industries and the health hazards caused by the effluents from these industries are increasingly reported in recent years. Hence, there is an immense need for the complete removal of these dyes from the contaminated water bodies using some effective techniques. The photocatalysis augmented by nanoparticle catalysts could be considered as a suitable method to meet such a need [10].

In the natural environment, degradation of dyes takes place spontaneously with the help of solar energy which is a composite of UV and IR irradiations. By way of utilizing these natural radiations and optimizing the experimental conditions, complete removal of dye pollutants could be achieved through M-NPs mediated photocatalytic degradation. Most of the earlier studies in the research area of remediation of organic dye pollution have explored the catalytic ability of nanocomposites or metal oxide nanoparticles on the degradation of selected dyes. Studies comparing the augmenting potentials of transition metal nanoparticles in the photocatalysis of organic dyes are scanty. Therefore, this study was carried out to explore the nanoparticles of Cu, Ni, and Ag for application as heterogeneous catalysts and to compare their efficacy in the photodegradation of three dyes in an aqueous medium at 25°C using $NaBH_4$ as the reductant.

EXPERIMENTAL

Synthesis and characterization of metal nanoparticles

To synthesize M-NPs, the wet chemical reduction method [20] was adopted with some modifications. Nanoparticles of copper, nickel, and silver metals were chemically synthesized by

reducing copper chloride ($CuCl_2.2H_2O$) / nickel chloride ($NiCl_2.6H_2O$) / silver nitrate ($AgNO_3$) with hydrazine hydrate ($N_2H_4.H_2O$) in the presence of stabilizing agents such as PEG (biopolymer) and PVP (synthetic polymer) individually. Ideally, Copper chloride/ nickle chloride / silver nitrate (0.350 g) and the polymeric stabilizer (0.25 g) were dissolved in a mixture of anhydrous ethanol (50 mL) and EG (50 mL) by ultrasonic dispersion for 30 – 40 min. Further, the mixture was heated to 70°C, during which the pH of the reaction solution was adjusted to 12.0 by dropwise addition of NaOH (0.1 M). Then, to the reaction solution hydrazine hydrate ($N_2H_4.H_2O$) ethanol solution (8 mL in 10 mL anhydrous ethanol) was added dropwise and heated up to 80°C for 4 hours along with constant stirring. The resultant M-NPs were cooled to room temperature and maintained in an anhydrous ethanol solution. Subsequently, the M-NPs were subjected to centrifugation, washed with anhydrous ethanol, and air-dried. The M-NPs thus prepared were stored in an airtight container purged with nitrogen (N_2) gas.

Characterization of M-NPs was performed using UV–visible spectrophotometry, FTIR, X-ray diffraction analysis, and electron microscopy coupled with EDX spectroscopy. UV–visible spectra analysis was performed for all samples and the absorption maxima were analyzed at a wavelength of 200–700 nm using UV–visible spectrophotometer. The synthesized M-NPs were subjected to FTIR examination to detect the biomolecules which could contribute towards efficient capping or stabilization. The crystalline nature of particles was evaluated by using the X-ray diffraction method (XRD) and the high-resolution transmission electron microscopy (HR-TEM) followed by dynamic light scattering (DLS) analysis to study the particle size, shape, and distribution of M-NPs. A detailed study on the morphology of M-NPs was carried out at room temperature (25±1°C) using scanning electron microscopy with a built-in field-emission (FE-SEM) gun operated at 200 kV. The elemental composition of M-NPs was analyzed with an energy-dispersive X-ray (EDX) spectroscopy equipment.

Batch experiment: Catalytic degradation of organic dyes

A One-pot decolorization reaction was chosen for carrying out dye degradation using a batch reactor. Stock solutions of different dyes (1mM; pH 7.0) viz., MB, BCG, and CV were prepared in deionized and double-distilled water. The typical experiment included a double-walled three-necked 100 mL glass round-bottomed flask fitted with a magnetic stirrer as a reactor. For each experiment, 0.5 mg of nanocatalyst was added to 20 mL of dye solution. Subsequently, the solution was mixed with freshly prepared aqueous 5% $NaBH_4$ (wt/v) solution. A Mercury lamp (120 W) was mounted on the top to serve as an artificial light source for UV light irradiation of the reaction mixture. A constant temperature of 25°C was maintained by circulation of water into the double-walled assembly. The reduction reaction was carried out for three days under vigorous stirring, and the progress was monitored using a UV-vis spectrophotometer. The absorbance at 664 nm for MB, 520 nm for BCG and 462 nm for CV were used to calculate the equilibrium adsorption of the dyes.

Aliquots of dye solution (0.5 mL) were drawn out at various time intervals for determining the parameters controlling the trend of decolorization for each dye system. Separate kinetic parameters were determined for solar and UV irradiations. A control experiment without the catalyst was also carried out.

A kinetic study of the decolorization was performed by measuring the wavelengths at maximum and decreased absorbance values for each of the dyes. The rate constants of the dye degradations were determined through recording absorbance variations with time i.e., 50% dye decomposition. Pseudo-first-order conditions were maintained by using ten times higher the value of reductant ($NaBH_4$) concentration than that of the dye. These values were calculated by multiplying constant 2.303 with the slopes of the linear kinetic plots generated. The pseudo-first-order rate coefficient values for the dye decolorization were determined from the kinetic plots which are obtained by plotting $\log(OD_0/OD_t)$ versus time. Catalytic efficiency (φ_c) of M-NPs were determined as follows: $\varphi_c = k_c/k_0$, where k_c and k_0 are the rates constant in the presence and absence of catalysts.

The effects of the bio stabilizer (PEG) and the synthetic polymeric stabilizer (PVP) on the nature of Cu, Ni, and Ag NPs catalyst systems were studied by determining the rate coefficient values of the decolorization of each of the dye system at constant pH.

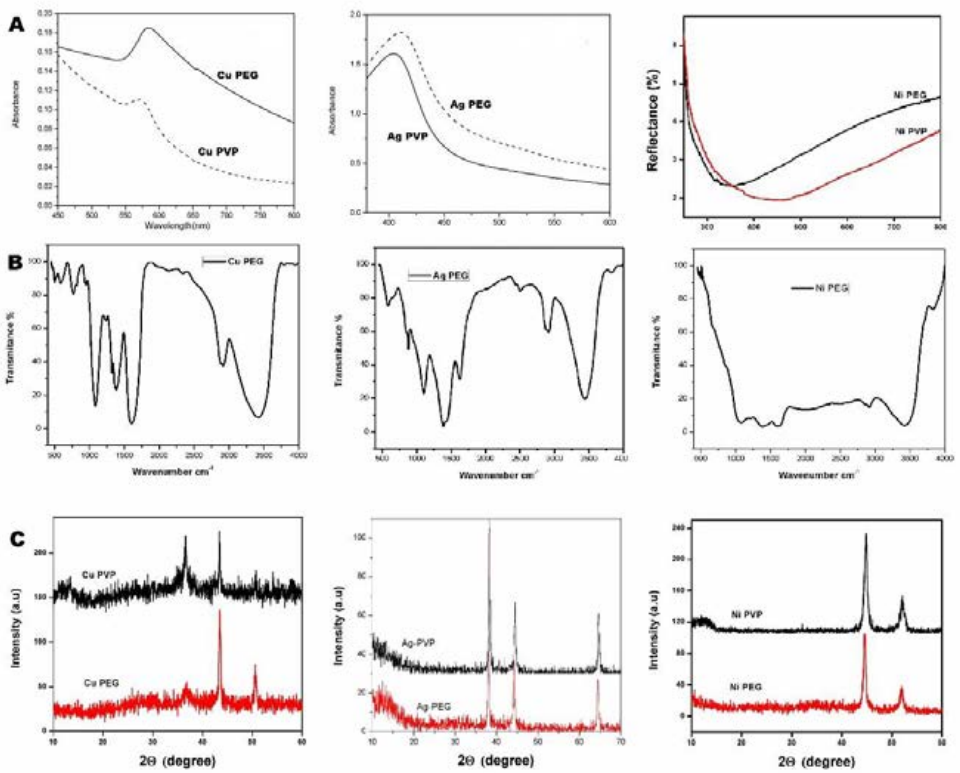

Fig. 1. Results of A) UV, B) FTIR and C) XRD analysis of Cu, Ag, and Ni nanoparticles

Assessment of mineralization of dyes

The mineralization processes of the dyes were ascertained by analyzing the treated dye solution for CO_2 generation and TOC removal. Production of CO_2 was determined by trapping the gaseous product of the reaction in a $Ba(OH)_2$ aqueous solution and gravimetrically estimating the resultant $BaCO_3$ precipitate. The TOC removal ratio (R) is defined as $R= (1- TOC_f/TOC_0) x100$, where TOC_0 and TOC_f are the TOC values at the initial and at any time t respectively.

RESULTS AND DISCUSSION

Characterization of M-NPs

Fig. 1A shows the UV–Vis spectra of nanoparticles of Cu, Ag, and Ni respectively. The maximum absorbance of Cu, Ni, and Ag nanoparticles was recorded at 380, 470, and 410nm respectively. The appearance of respective peaks corresponding to the surface plasmon resonance (SPR) bands is a formation index of M-NPs during the reaction [21]. The formation of SPR is due to the particle shape, size, interaction with the medium, and the degree of charge transfer between the particle and the medium [22].

The FTIR spectra (Fig. 1B) indicated intense bands corresponding to H-bonded O-H stretch at 1583, 3247, and 2832 cm^{-1} respectively for Cu, Ni, and Ag-NPs. Bands corresponding to C-O stretch were recorded at 1892, 3558, and 2941 cm^{-1} for respective M-NPs. Peak bands of C=C stretch for respective M-NPs were observed at 997, 1075, and 1836 cm^{-1}. Occurrences of C-F strong stretch in each of the M-NPs were indicated by the bands formed at 1275, 1573, and 1244 cm^{-1}. These values are similar to those recorded in the studies carried out by Muthukrishnan et al. [22]. The IR spectrum analysis also provided an idea about biomolecules bearing different functionalities which are present in the basic system [23]. The broad SPR bands indicating nucleation of M-NPs and growth on capping agents appeared with minimum exposure times of 130, 180, and 145 minutes respectively for Cu, Ni, and Ag-NPs.

The X-ray diffraction analysis of M-NPs confirmed that the particles were of pure phase and crystalline in nature (Fig. 1C). Distinct Bragg reflections corresponding to lattice planes of

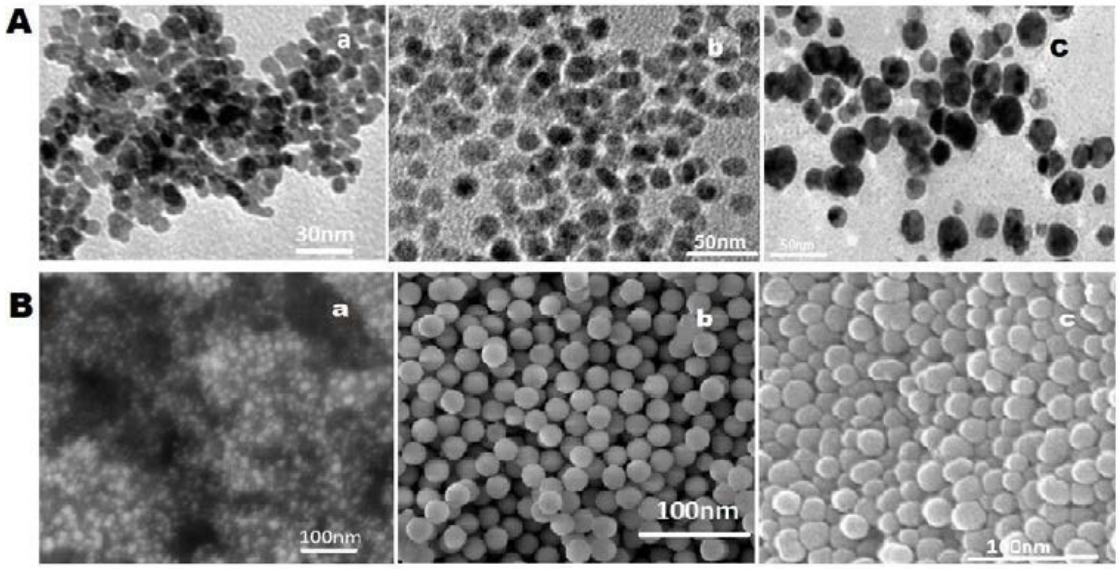

Fig. 2. Micrographs of A) TEM and B) SEM of Cu (a), Ag (b), and Ni (c) nanoparticles

specific shapes of each M-NPs were observed. The 2θ values of 33.4., 45.5, 58.3, 67.1, and 77.3 correspondings to the (125), (228), (105), (126) and (303) planes were observed for Cu-NPs. For Ni- NPs the 2θ values were 32, 34.5, 46, 52.4, 55.8 and 61.7° corresponding to the (218), (313), (405), (429), (521) and (438) planes. Diffraction peaks allocated at 38.2°, 44.7°, 57.6°, and 65.2° for appropriate lattice planes (109), (207), (225), and (315) were corresponding to the Ag- NPs. Besides, unassigned peaks occurred due to changes on the nanoparticle surface leading to crystallization of the organic phase [24].

The TEM micrographs showed that while the particles of Cu and Ag were spherical to cubic, uniform, and homogeneous in morphology, the Ni-NPs were polycrystalline (Fig. 2). Furthermore, it was also noted that the particles were discrete and non-agglomerated. In agreement with our study, Mntungwa et al. [25] and Basu et al. [26] from their independent studies reported that the M-NPs were spherically shaped with no agglomeration. Dynamic light scattering (DLS) analysis to record the size distribution of M- NPs was carried out using Analysette 22 NeXT automatic particle size analyzer (Germany). DLS pattern was in correlation with TEM values and indicated the occurrence of cubic particles with a narrow size distribution in ranges of 3-25 nm (Cu-NPs) , 7-38 nm (Ni-NPs), and 4-45 nm (Ag-NPs). The polydispersity index (PI) values determined for Cu, Ni, and Ag- NPs respectively were 0.6, 0.8, and 0.9. The average size of the M-NPs were calculated based on the size equal to that of nanoparticles of >75% of occurrence. The average particle sizes calculated for Cu, Ni, and Ag-NPs synthesized using PEG respectively were 12±1 nm, 18±1 nm, and 15±1 nm, while the sizes of the same synthesized using PVP respectively were 15±1 nm, 22±1 nm, and 20±1 nm. The presence of stabilizers could be attributed to the inhibition of agglomeration of M-NPs. Distinct shapes of M-NPs were further confirmed using FESEM (Fig. 2). The EDX profile showed characteristic peaks for elements C, H, O, and Ni, etc. present in the M-NPs. The EDX spectrum depicted the energy bands centered at 3.7, 8.2, and 7.3 keV respectively of Cu, Ni, and Ag-NPs. Fayaz et al. [27] have reported that occurrences of these peaks are an index of proper synthesis of M-NPs.

Photocatalytic degradation experiment

The feasibility of the synthesized M-NPs as potential catalysts for removal of dyes was studied using three commonly used dyes. When dyes were used with an initial concentration of 1mM, almost 80% of anionic dyes (BCG and CV) were removed in 90-120 minutes, whereas 80% of the cationic dye (MB) was removed favorably in 30-60 minutes. In particular, MB - a water-soluble thiazine cationic dye assumes an absorption maximum at 665 nm when it is in an oxidized form. The action of reducing agents such as $NaBH_4$ causes its fading

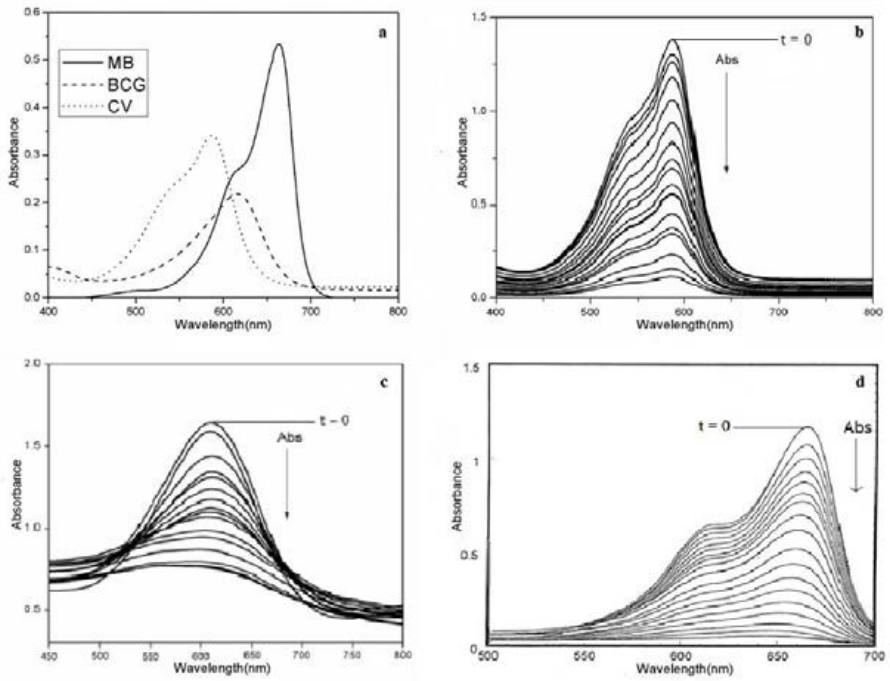

Fig. 3. UV VIS spectra of a) Typical curves and Stacked curves of variation with time for reduced b) CV, c) BCG and d) MB dyes

into a colorless form called, leuco-methylene blue (LMB) [28,29].

It was found that, when the dye solutions were mixed with $NaBH_4$ (2% wt/v) and kept for more than 24 hours, only <5% decolorization occurred from the initial color intensity. When M- NPs were added to $NaBH_4$ mixed dye solutions, nearly in four hours, complete fading of the color was achieved. Although $NaBH_4$ could serve as a reductant [28,29], photo energy is decisive for of degradation of dye contaminated effluents in the natural environment [30]. In line with our findings, Ayodhya and Veerabhadram [30] have demonstrated a superior rate of $NaBH_4$ – CdS- NPs mediated degradation of MB dye under light (97%) than that carried out without any irradiation (<50%).

The UV vis spectra of the treated dyes (Fig. 3) indicated that the absorbance maxima (λmax) of the dye solutions diminished after the treatment process. The relative absorbance bands (λmax) for MB, BCG, and CV in samples were observed at 625, 590, and 610 nm respectively. There was a gradual reduction in these absorbance values after 30 min of the addition of Cu, Ni, and Ag-NPs to the dye. In parallel, a proportionate increase of SPR of M-NPs was also observed. The ability of M-NPs to degrade the dyes was indicated by a decrease in absorbance values. Concomitant with our observation, Bhakya et al. [8], in their study on photocatalytic reduction of methyl violet (MV) using Ag- NPs, found that there was a marked decrease of absorbance and increase of SPR peaks at the end of 30 min of treatment.

Ramalingam et al. [31] suggested that at lower pH ranges, due to electrostatic interactions, the adsorption property of M-NPs increases. In contrast to this view, Saeed et al. [32] have reported that the alkaline conditions are more favorable for dye degradation as the preponderance of OH· radicals occurs especially in higher pH values. Studies have suggested that the low and high pH ranges of the medium have an augmenting effect on the adsorption property of M-NPs [31,32]. However, the present study did not observe any changes in the rate of reactions proportionate with the pH of the medium. The entire process was carried out at a constant pH of 7.0. In our study, a constant temperature of 25°C was maintained throughout the degradation process. and interestingly, any temperature change did not have a significant influence on the reaction. Gupta et al. [33] believe that photocatalytic reactions are less temperature-dependent.

Our study identified certain parameters such as

shape, size, and quantity of M-np catalysts, initial concentration of dye, and contact time of catalysts with dye solutions as significant factors influencing the photocatalytic degradation of dyes.

The M-NPs of cubic shape happened to possess sharp corners and edges and encompass a higher fraction of atoms. As these atoms would be chemically active and likely to dissolve easily, these regions serve for profuse catalytic activities of the M-NPs [29]. Our study found that this concept is agreeable as the Cu- and Ag-NPs, which are cubic, demonstrated better degradative ability (95%) than the Ni-NPs (85%).

The rate of photocatalytic reactions would be directly proportional to the quantity of M-NPs catalysts [34]. This is evident from our study that the Cu-PEG-NPs at a concentration of 0.5mg caused instant fading of color with the removal of 80% of dye within 10 min unlike the same in lower concentrations.

The size of the M-NPs has a direct impact and would be indirectly proportional to the catalytic activity in the degradation of organic dyes [35]. Particles with smaller sizes tend to favor higher proliferation and coordination of atoms on their surfaces which in turn facilitates better adsorption and degradation of dyes [35]. In conform to this theory, our study observed that smaller particles such as Cu-NPs (12-15±1 nm) and Ag-NPs (15-20±1 nm) possess more catalytic efficiency than the larger particles i.e., Ni-NPs (18-22±1 nm).

The initial concentration of dye in the experiment is also a critical parameter in the photocatalytic degradation. In our study, an initial concentration of 1mM of each dye was used for degradation experiments which warranted about 4h for complete degradation. Higher concentrations of dyes usually hinder the penetration of radiations to the surface of catalysts and hence reduce the rate of reaction [32]. This has been evident from the studies of Saeed et al. [32], who demonstrated that the rate of photocatalytic degradation of Rhodamine B and MB dyes by Ag-Co_3O_4 nanocomposites decreased from 97% to 60% when the concentration of dyes was increased from 100 mg/mL to 300 mg/mL.

The contact time of catalysts (solid phase) with the dye solution (liquid phase) is a critical factor for the successful application of photocatalysis in the real treatment of wastewater. Indeed, the contact time promotes the exposure of reactive sites and adsorption of dyes onto the nanocatalysts [34]. In the present study, although the decolorization of dyes began within 5-15 min, acceleration of degradation was observed proportionate with the length of time. However, the rate of catalysis became stabilized after 4h of treatment. Concomitant with our findings Meva et al. [36], who investigated the application of Cu-NPs for degradation of MB, methyl orange, and eosin Y in aqueous solution, have reported the initial increasing trend of dye degradation and attainment of equilibrium with the extension of contact time.

Degradation kinetic studies

Typical UV-Vis spectra of the three dyes are shown in Fig. 3. The present study explains the absorbance versus time kinetics about photocatalytic degradation of three dyes with reference to the reaction catalyzed by Cu-NPs for convenience. This is mainly because the pattern of reactions catalyzed by all the M-NPs was more or less similar. Figs. 4 and 5 depict absorbance versus time variance plots for the degradation of three dye systems catalyzed respectively by PEG and PVP stabilized Cu, Ag, and Ni-NPs. As the reaction proceeded, the absorbance maxima (λmax) of each of the dyes diminished with time. A recent work by Saeed et al. [37] on the photocatalytic degradation of methyl orange using Ag-TiO2 reported a similar observation.

The reaction parameters such as the rate coefficient values (k), the half-life periods (t_{50}%), and catalytic efficiency (φ_c) that are determined for the degradation of dyes carried out in presence of PEG capped Cu-NPs catalysts independently under solar and UV irradiations are presented in Table 1.

Solar irradiation is composite and contains a larger portion of UV irradiation and a smaller portion of IR irradiation. While the IR irradiation causes heating effects, the UV radiation is responsible for augmenting the catalytic property of M-NPs in aqueous solutions. However, the rate coefficient for catalysis was comparatively inferior when UV light was used separately as a source of irradiation. The derived k values, as recorded in our study (Table 1), inferred that Cu-PEG-NPs catalyzed the reaction better under solar irradiation than the UV irradiation. Comparative study of φ_c values deciphered the trend of catalytic efficiency regarding the irradiations as solar > UV irradiation. The superior performance of solar radiations could be because of the presence of higher intensity of UV in solar photolysis than that of sole UV irradiations. The yellow light in the solar radiation contributes

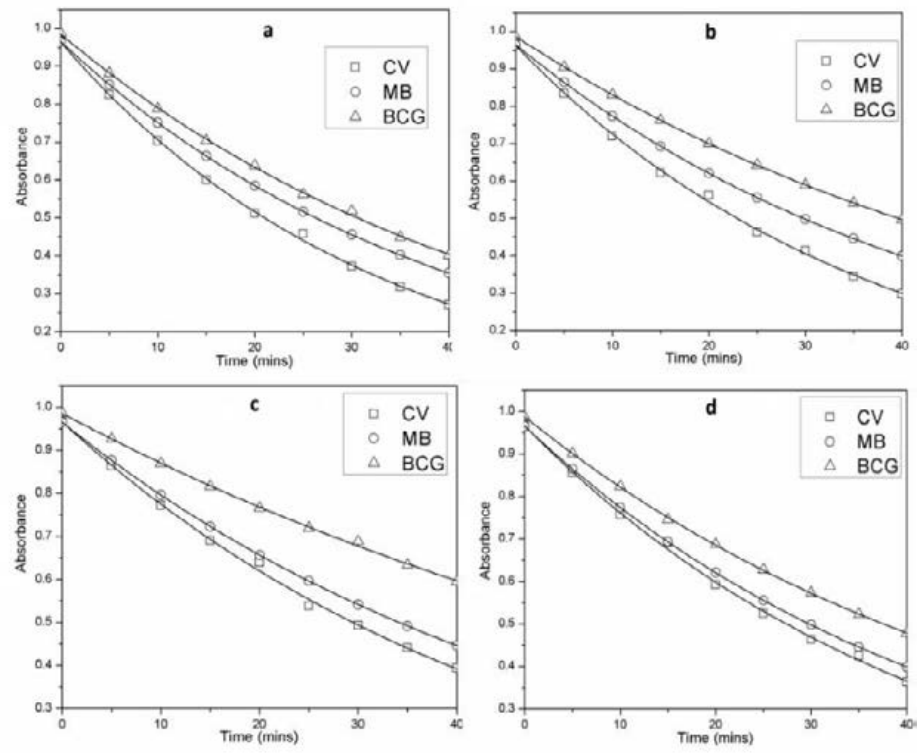

Fig. 4. Absorbance vs Time plots for the reductive degradation of three dyes catalyzed by a) Cu-PEG-NPs b) Ag-PEG-NPs c) Ni-PEG-NPs under solar irradiation and d) Cu-PEG-NPs under UV irradiation.

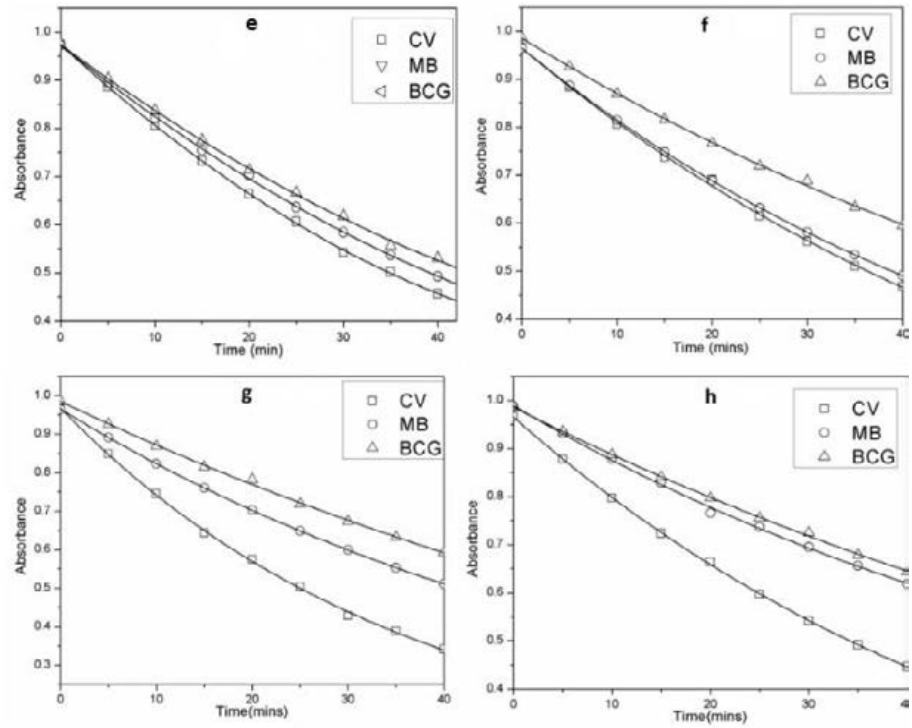

Fig. 5. Absorbance vs Time plots for the reductive degradation of three dyes catalyzed by e) Cu-PVP-NPs under solar irradiation f) Cu-PVP-NPs g) Ag-PVP-NPs h) Ni-PVP-NPs under UV irradiation.

Table 1. Rate coefficient (k) values, times of 50% reduction, and catalytic efficiency(φ_c) under pseudo-first-order conditions determined for the reduction of dyes using $NaBH_4$ and Cu-PEG-NPs

Entry	Dyes	Solar irradiation			UV irradiation		
		k ($x10^{-4}$) s^{-1}	$t_{50\%}$ min	φ_c	k ($x10^{-4}$) s^{-1}	$t_{50\%}$ min	φ_c
1	CV	5.30	21	8.70	4.86	24	7.89
2	MB	4.17	27	7.71	3.71	31	5.81
3	BCG	3.75	30	6.03	3.22	35	3.84

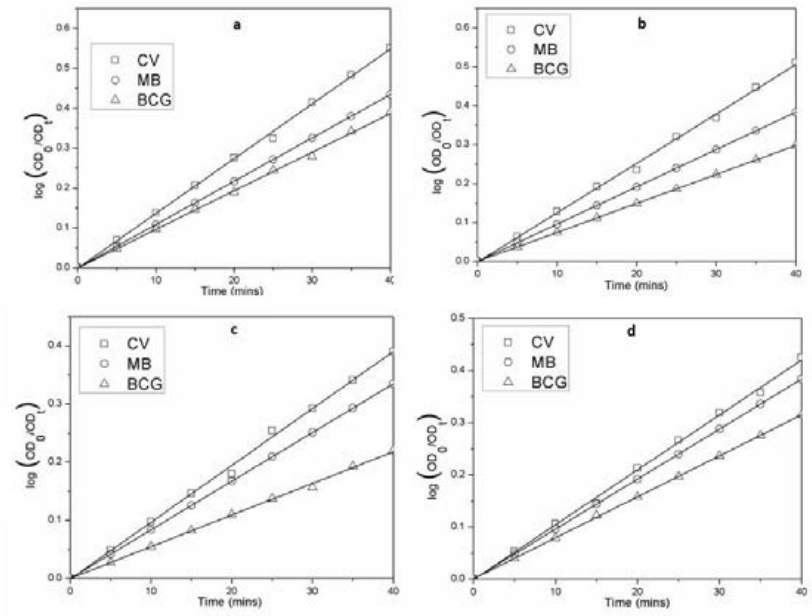

Fig. 6. Kinetic plots for the reductive degradation of three dyes catalyzed by a) Cu-PEG- NPs b) Ag-PEG-NPs c) Ni-PEG-NPs under solar irradiation and d) Cu-PEG-NPs under UV irradiation.

to the catalysis of the reductive degradations of dye by M-NPs.

Figs. 6 and 7 show the kinetic plots of M-NPs for the catalytic degradation of three dye systems under solar and UV irradiations respectively by PEG and PVP stabilized M-NPs. The kinetic plots (Figs. 6 & 7) exhibit pseudo-first-order kinetic concerning the irradiation time and absorbance and demonstrated their linear relationship in the degradation of dyes. It may be noted that a gradual exponential decrease in the absorbance values with the time occurred during the reaction. A similar study conducted on the degradation of organic dyes using Ag-NPs by Bhakya et al. [8] explained that the linear correlation between the absorbance values (A/A0) with the reaction time is an index of pseudo-first-order for the reduction of dyes.

The rate coefficient values for the degradation of the three dyes catalyzed by both PEG and PVP stabilized M-NPs independently under UV and solar photo irradiations are given in Table 2. Comparison of k-values indicated that the trend of catalytic efficiency of M-NPs in the degradation of three dyes systems was Cu>Ag>Ni-nps (Table 2). It is a well-known fact that under constant compositions, smaller sized particles produce larger surface area encompassing higher active sites. Our study documented that the catalytic efficiency is inversely proportional to the size of M-NPs through recording the superior and inferior rate coefficient values produced by small-sized Cu-NPs and large-sized Ni-NPs. Besides, in terms of causing the synthesis of smaller sized particles, the PEG was observed to a better stabilizer than PVP.

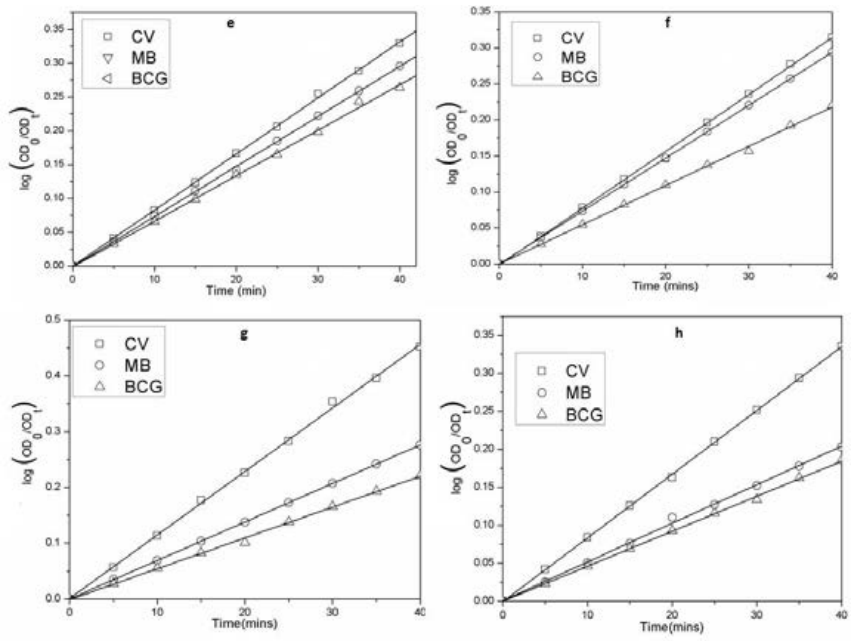

Fig. 7. Kinetic plots for the reductive degradation of three dyes catalyzed by e) Cu-PVP-NPs under solar irradiation f) Cu-PVP-NPs g) Ag-PVP-NPs h) Ni-PVP-NPs under UV irradiation.

Table 2. Rate coefficient k ($x10^{-4}$ s^{-1}) values under pseudo-first-order conditions determined for the reduction of dyes using $NaBH_4$ and Cu, Ni and Ag-NPs with PEG, and PVP stabilizing agents

Dyes	SOLAR IRRADIATION						UV IRRADIATION					
	PEG			PVP			PEG			PVP		
	Cu-NPs	Ag-NPs	Ni-NPs	Cu-NPs	Ag-NPs	Ni-NPs	Cu-NPs	Ag-NPs	Ni-NPs	Cu-NPs	Ag-NPs	Ni-NPs
CV	5.30	4.08	3.82	4.91	3.74	3.02	4.86	3.68	3.23	3.75	3.22	2.95
MB	4.17	3.68	3.05	3.61	3.21	2.82	3.71	3.00	2.65	2.90	2.65	1.95
BCG	3.75	3.02	2.66	3.23	2.76	2.11	3.22	2.82	1.95	2.62	2.12	1.78

Comparing the nanoparticle sizes and keeping all conditions constant, the trend in catalytic reactions regarding the stabilizers was PVP<PEG.

Mineralization of dyes

The ultimate result of the decolorization of dyes is mineralization [10]. In some cases, the partial transformation of the dyes to CO_2 have been reported [23]. Treatment of dyes using $NaBH_4$ as the reductant without a catalyst, although complete bleaching of the color takes place, may cause the release of some incompletely degraded organic products. Under constant conditions at 25°C, a 20 mL of 1mM solution of the dye produced 0.2g of $BaCO_3$ corresponding to 92% of carbon released as CO_2 after two hours.

Preliminary studies on the effect of concentration of $NaBH_4$ on the catalyst incorporated dye solutions indicated that, although a 5% (w/v) of reductant caused instant decolorization, no change in the reaction was observed with further increase in concentration. Pal et al. [38] suggested that the

Table 3. TOC removal ratio (R) on the mineralization of MB, CV, and BCG with Cu-PEG NPs at 25°C under solar irradiation

Entry	Nanoparticles	CV		MB		BCG	
		R^a(%)	R^b(%)	R^a(%)	R^b(%)	R^a(%)	R^b(%)
1	PEG-Cu-NPs	94	93	91	90	90	88
2	PVP-Cu-NPs	92	90	89	87	87	86

[a] [dye]= 1mM; [b] [dye] = 0.7mM

reduction of dyes is solely dependent on catalysts despite the excessive presence of a reductant.

Mineralization of dyes to CO_2 and H_2O depends not only on the reaction time allowed but also on the nature of the M-NPs used [38]. In table 3, the TOC values of degradation reactions carried out by Cu-NPs catalysts with two different initial concentrations of the dye are summarized. Keeping the concentrations of reductants constant, for 30 min of reaction conditions higher R values were obtained with the catalysts stabilized with PEG than those with PVP. For 85% of TOC removal ratio, the least time of reaction was recorded for PEG stabilized Cu-NPs catalyst system. Under constant experimental conditions, for any one of the three dye systems, the catalytic efficiency of M-NPs based on the nature of the stabilizer was observed to be PEG>PVP**.** This trend observed could be rationalized as PEG facilitates the production of smaller sized nanoparticles with a larger surface area than PVP stabilizers. Structural implications such as the presence of more of –OH groups in PEG than in PVP stabilizers can be invoked for such a trend.

Considering the R values for 85% of TOC removal at a constant time of reaction, the trend of catalysis by Cu-NPs for the dye systems was CV > MB > BCG. Owing to the possession of three para alkyl amino substitutions, the CV showed rapid decolorization. On the other hand, the BCG dye, due to the presence of Bromo ring substitution along with the sulphonate group, consumed a longer time for decolorization.

Reaction pathway

Generally, the reduction reaction is the basis for the degradation of dye molecules. The degradation of dyes catalyzed by M-NPs, in the presence of $NaBH_4$, could be explained by Eley–Rideal (E-R) adsorption mechanism. The photocatalytic degradation of dyes is based on the formation of electrons and holes on the nanoparticle catalyst under the influence of irradiation [39]. The M-NPs usually act as a substrate for adsorption of reductants on their surface and catalyze the e-relay reactions between the donor and the acceptor [40].

The presence of $NaBH_4$ in aqueous solutions causes the release of borohydride (BH_4^-) ions. Using electrostatic attraction the BH_4^- ions are adsorbed onto the M-NPs, which makes their surface negatively charged.

$\{BH_4^- + 3H_2O \rightarrow BO_3^{3-} + 8\ e^- + 10\ H^+\}$

The photo-assisted reaction causes electron-hole pairs on the surface of nanoparticles between conduction and valence band [41]. This prompts the M-NPs to transfer the electrons to the dye molecules, thus initiating the reduction reaction. As the negative layered M-NPs attract more extents of dye molecules, a facile breakdown of the dye occurs over the surface of M-NPs due to the facilitation of intramolecular H-bonding in the dye. Besides, the nascent hydrogen species generated from BH_4^- ions attack the dye that has been concentrated at the electron-rich sites of the molecule. Thus, the presence of heteroatoms and electron transfer from the negatively charged particles enhances the overall rate of the reaction. All these mechanisms together enhance the mineralization of the dye molecules. Veerakumar et al. [34], from their studies on the degradation of organic dyes using Ni-NPs -decorated porous carbon, have proposed that the two-electron transfer processes taking place on the surface of M-NPs play a significant role in the photocatalytic reduction of dyes.

Our study recorded higher rate coefficient values of M-NPs concerning the degradation of dyes when carried out under UV irradiation than that of solar irradiation. This implies that UV radiation plays a crucial role in facilitating the formation of electron-hole pairs. Concomitant with our finding, recently Mohan and Devan [24] have demonstrated that the safranin O dye contaminated textile effluent was best treated using Ag-Ni bimetallic nanoparticles under UV light irradiations.

CONCLUSIONS

Metal nanoparticles serve as potential catalysts for photocatalytic degradation of dyes and augment

the action of $NaBH_4$ for the reduction reaction. Degradation is primarily dependent on catalysts and an increase in the concentration of reductant has no bearing on the reaction. The M-NPs are more efficient in causing the degradation (≥80%) of cationic dye MB than with anionic dyes MB and BCG. There is a linear relationship between the irradiation time and absorbance and the reactions abide by pseudo-first-order kinetic photocatalytic degradation of dyes. Mineralization of dyes depends not only on the reaction time allowed but also on the nature of the M-NPs used. M-NPs of cubic shape, smaller size, and of higher quantity has a positive effect on photocatalysis. The initial concentration of the dye and contact time of M-NPs are the critical factors for the photodegradation of dyes. Significant catalysis by M-NPs takes place at a pH and temperature of 7.0 and 25°C respectively of the medium, and the changes in these values do not affect the reaction.

The trend of reactions concerning catalytic efficiency (j_c) values of M-NPs in the degradation of three dyes systems is Cu>Ag>Ni-nps and is inversely proportional to the size of M-NPs (Cu<Ag<Ni NPs). The PEG serves as a better stabilizer than PVP in terms of causing the production of smaller M-NPs and more –OH groups. Comparing the nanoparticle sizes and keeping all conditions constant, the trend in catalytic reactions concerning the stabilizers was PVP<PEG. In terms of rate coefficient (k) values of M-NPs and the impact of source of photo energy, the trend of dye degradation is solar > UV irradiation. Formation of electron-hole pair on the surface of catalyst facilitated by radiation is the key process in the reductive degradation of dyes.

ACKNOWLEDGEMENTS

The authors thank the Department of Nanoscience and Technology, University of Madras for providing the necessary equipment facility for performing characterization studies on nanoparticles.

DECLARATION

The authors declare that there are no conflicts of interest.

REFERENCES

1. Sen TK, Afroze S, Ang HM. Equilibrium, Kinetics and Mechanism of Removal of Methylene Blue from Aqueous Solution by Adsorption onto Pine Cone Biomass of Pinus radiata. Water, Air, & Soil Pollution. 2010;218(1-4):499-515.
2. Al-Amrani WA, Lim P-E, Seng C-E, Wan Ngah WS. Factors affecting bio-decolorization of azo dyes and COD removal in anoxic–aerobic REACT operated sequencing batch reactor. Journal of the Taiwan Institute of Chemical Engineers. 2014;45(2):609-16.
3. Soler L, Sánchez S. Catalytic nanomotors for environmental monitoring and water remediation. Nanoscale. 2014;6(13):7175-82.
4. Faisal M, Abu Tariq M, Muneer M. Photocatalysed degradation of two selected dyes in UV-irradiated aqueous suspensions of titania. Dyes and Pigments. 2007;72(2):233-9.
5. Xie Y, Yan B, Xu H, Chen J, Liu Q, Deng Y, et al. Highly Regenerable Mussel-Inspired Fe3O4@Polydopamine-Ag Core–Shell Microspheres as Catalyst and Adsorbent for Methylene Blue Removal. ACS Applied Materials & Interfaces. 2014;6(11):8845-52.
6. Muthirulan P, Nirmala Devi C, Meenakshi Sundaram M. Synchronous role of coupled adsorption and photocatalytic degradation on CAC–TiO 2 composite generating excellent mineralization of alizarin cyanine green dye in aqueous solution. Arabian Journal of Chemistry. 2017;10:S1477-S83.
7. Sharma MK, Sobti RC. Rec effect of certain textile dyes in Bacillus subtilis. Mutation Research/Genetic Toxicology and Environmental Mutagenesis. 2000;465(1-2):27-38.
8. Muthukrishnan S BS, Muthukumar M SM, Rao Mv SKT. Catalytic Degradation of Organic Dyes using Synthesized Silver Nanoparticles: A Green Approach. Journal of Bioremediation & Biodegradation. 2015;06(05).
9. Tang WZ, Huren A. UV/TiO2 photocatalytic oxidation of commercial dyes in aqueous solutions. Chemosphere. 1995;31(9):4157-70.
10. Ghosh SK, Kundu S, Mandal M, Pal T. Silver and Gold Nanocluster Catalyzed Reduction of Methylene Blue by Arsine in a Micellar Medium. Langmuir. 2002;18(23):8756-60.
11. Ata S, Shaheen I, Qurat ul A, Ghafoor S, Sultan M, Majid F, et al. Graphene and silver decorated ZnO composite synthesis, characterization and photocatalytic activity evaluation. Diamond and Related Materials. 2018;90:26-31.
12. Arshad M, Abbas M, Ehtisham-ul-Haque S, Farrukh MA, Ali A, Rizvi H, et al. Synthesis and characterization of SiO2 doped Fe2O3 nanoparticles: Photocatalytic and antimicrobial activity evaluation. Journal of Molecular Structure. 2019;1180:244-50.
13. So CM, Cheng MY, Yu JC, Wong PK. Degradation of azo dye Procion Red MX-5B by photocatalytic oxidation. Chemosphere. 2002;46(6):905-12.
14. Han F, Kambala VSR, Srinivasan M, Rajarathnam D, Naidu R. Tailored titanium dioxide photocatalysts for the degradation of organic dyes in wastewater treatment: A review. Applied Catalysis A: General. 2009;359(1-2):25-40.
15. Nezamzadeh-Ejhieh A, Moeinirad S. Heterogeneous photocatalytic degradation of furfural using NiS-clinoptilolite zeolite. Desalination. 2011;273(2-3):248-57.
16. Zabihi-Mobarakeh H, Nezamzadeh-Ejhieh A. Application of supported TiO2 onto Iranian clinoptilolite nanoparticles in the photodegradation of mixture of aniline and 2, 4-dinitroaniline aqueous solution. Journal of Industrial and Engineering Chemistry. 2015;26:315-21.
17. Ahmed S, Rasul MG, Brown R, Hashib MA. Influence of parameters on the heterogeneous photocatalytic degradation of pesticides and phenolic contaminants in wastewater: A short review. Journal of Environmental

Management. 2011;92(3):311-30.
18.Beydoun D, Amal R, Low G, McEvoy SJ. Role of nanoparticles in photocatalysis. *J Nanopart Res*, 1999; 1(4): 439-458.
19. Nadagouda MN, Varma RS. Green synthesis of silver and palladium nanoparticles at room temperature using coffee and tea extract. Green Chemistry. 2008;10(8):859.
20.Sun Y and Xia Y. Shape controlled synthesis of gold and silver nanoparticles. *Science*, 2002; 298: 2176-79.
21. Das SK, Khan MMR, Guha AK, Das AR, Mandal AB. Silver-nano biohybride material: Synthesis, characterization and application in water purification. Bioresource Technology. 2012;124:495-9.
22. Muthukrishnan S, Bhakya S, Senthil Kumar T, Rao MV. Biosynthesis, characterization and antibacterial effect of plant-mediated silver nanoparticles using Ceropegia thwaitesii – An endemic species. Industrial Crops and Products. 2015;63:119-24.
23.Zhu M, Dia G. Synthesis of Porous Fe3O4 Nanospheres and Its Application for the Catalytic Degradation of Xylenol Orange. *J Phys Chem C*, 2011; 115: 18923-34.
24. Mohan S, Devan MV. Photocatalytic activity of Ag/Ni bi-metallic nanoparticles on textile dye removal. Green Processing and Synthesis. 2019;8(1):895-900.
25. Mntungwa N, Pullabhotla VSR, Revaprasadu N. Facile Synthesis of Organically Capped CdTe Nanoparticles. Journal of Nanoscience and Nanotechnology. 2012;12(3):2640-4.
26. Basu S, Maji P, Ganguly J. Rapid green synthesis of silver nanoparticles by aqueous extract of seeds of Nyctanthes arbor-tristis. Applied Nanoscience. 2015;6(1):1-5.
27. Fayaz AM, Balaji K, Girilal M, Yadav R, Kalaichelvan PT, Venketesan R. Biogenic synthesis of silver nanoparticles and their synergistic effect with antibiotics: a study against gram-positive and gram-negative bacteria. Nanomedicine: Nanotechnology, Biology and Medicine. 2010;6(1):103-9.
28. Zhang Y, Zhu P, Chen L, Li G, Zhou F, Lu D, et al. Hierarchical architectures of monodisperse porous Cu microspheres: synthesis, growth mechanism, high-efficiency and recyclable catalytic performance. Journal of Materials Chemistry A. 2014;2(30):11966.
29. Li X-Z, Wu K-L, Ye Y, Wei X-W. Controllable synthesis of Ni nanotube arrays and their structure-dependent catalytic activity toward dye degradation. CrystEngComm. 2014;16(21):4406-13.
30. Ayodhya D, Veerabhadram G. One-pot green synthesis, characterization, photocatalytic, sensing and antimicrobial studies of Calotropis gigantea leaf extract capped CdS NPs. Materials Science and Engineering: B. 2017;225:33-44.
31. Ramalingam B, Khan MMR, Mondal B, Mandal AB, Das SK. Facile Synthesis of Silver Nanoparticles Decorated Magnetic-Chitosan Microsphere for Efficient Removal of Dyes and Microbial Contaminants. ACS Sustainable Chemistry & Engineering. 2015;3(9):2291-302.
32. Saeed M, Muneer M, Mumtaz N, Siddique M, Akram N, Hamayun M. Ag-Co 3 O 4 : Synthesis, characterization and evaluation of its photo-catalytic activity towards degradation of rhodamine B dye in aqueous medium. Chinese Journal of Chemical Engineering. 2018;26(6):1264-9.
33. Gupta VK, Jain R, Mittal A, Saleh TA, Nayak A, Agarwal S, et al. Photo-catalytic degradation of toxic dye amaranth on TiO2/UV in aqueous suspensions. Materials Science and Engineering: C. 2012;32(1):12-7.
34. Veerakumar P, Chen S-M, Madhu R, Veeramani V, Hung C-T, Liu S-B. Nickel Nanoparticle-Decorated Porous Carbons for Highly Active Catalytic Reduction of Organic Dyes and Sensitive Detection of Hg(II) Ions. ACS Applied Materials & Interfaces. 2015;7(44):24810-21.
35. Falicov LM, Somorjai GA. Correlation between catalytic activity and bonding and coordination number of atoms and molecules on transition metal surfaces: Theory and experimental evidence. Proceedings of the National Academy of Sciences. 1985;82(8):2207-11.
36.Meva FE, Ndom JC, Yonga AW, Ntoumba AA, Kedi PBE, Loudang REN, Segnou ML, Mang RE, Mbeng JOA, Mpondo EAM, Mbaze LM. Synthesis of copper nanoparticles mediated *Musanga cecropioides* leaf extract and their application in the degradation of organic dyes. *Int J Green Herb Chem*, 2017; 6(4): 280-290.
37. Saeed M, Muneer M, Khosa MKK, Akram N, Khalid S, Adeel M, et al. Azadirachta indica leaves extract assisted green synthesis of Ag-TiO2 for degradation of Methylene blue and Rhodamine B dyes in aqueous medium. Green Processing and Synthesis. 2019;8(1):659-66.
38. Pal J, Ganguly M, Dutta S, Mondal C, Negishi Y, Pal T. Hierarchical Au–CuO nanocomposite from redox transformation reaction for surface enhanced Raman scattering and clock reaction. CrystEngComm. 2014;16(5):883-93.
39. Rostami-Vartooni A, Nasrollahzadeh M, Salavati-Niasari M, Atarod M. Photocatalytic degradation of azo dyes by titanium dioxide supported silver nanoparticles prepared by a green method using Carpobrotus acinaciformis extract. Journal of Alloys and Compounds. 2016;689:15-20.
40. Christopher P, Xin H, Linic S. Visible-light-enhanced catalytic oxidation reactions on plasmonic silver nanostructures. Nature Chemistry. 2011;3(6):467-72.
41. Rahman QI, Ahmad M, Misra SK, Lohani M. Effective photocatalytic degradation of rhodamine B dye by ZnO nanoparticles. Materials Letters. 2013;91:170-4.